Denaturation of circular DNA: Supercoils and overtwist

Amir Bar,[1,2] Alkan Kabakçıoğlu,[3] and David Mukamel[1]
[1]*Department of Physics of Complex Systems, The Weizmann Institute of Science, Rehovot 76100, Israel*
[2]*Department of Computer Science and Applied Mathematics, The Weizmann Institute of Science, Rehovot 76100, Israel*
[3]*Department of Physics, Koç University, Sarıyer 34450 İstanbul, Turkey*
(Received 30 July 2012; published 11 December 2012)

The denaturation transition of circular DNA is studied within a Poland-Scheraga-type approach, generalized to account for the fact that the total linking number (LK), which measures the number of windings of one strand around the other, is conserved. In the model the LK conservation is maintained by invoking both overtwisting and writhing (supercoiling) mechanisms. This generalizes previous studies, which considered each mechanism separately. The phase diagram of the model is analyzed as a function of the temperature and the elastic constant κ associated with the overtwisting energy for any given loop entropy exponent c. As in the case where the two mechanisms apply separately, the model exhibits no denaturation transition for $c \leqslant 2$. For $c > 2$ and $\kappa = 0$ we find that the model exhibits a first-order transition. The transition becomes of higher order for any $\kappa > 0$. We also calculate the contribution of the two mechanisms separately in maintaining the conservation of the linking number and find that it is weakly dependent on the loop exponent c.

DOI: 10.1103/PhysRevE.86.061904 PACS number(s): 87.15.Zg, 36.20.Ey

I. INTRODUCTION

The thermal denaturation of DNA, whereby the two strands of the molecule separate upon heating, has been thoroughly investigated both experimentally and theoretically in the last half century. This process is relevant for experiments such as polymerase chain reaction (PCR) [1,2], and for biological processes such as those taking place within a thermophilic bacteria [3,4]. The fraction of bound base pairs vs temperature (the melting curve) can be measured by means of UV absorbtion [5,6]. Fluorescence techniques are also used for measuring the melting curve [7] and the lifetime of denatured loops [8–11] in short DNA structures such as hairpins and primers.

A typical melting curve of chains of the order of thousands of base pairs is composed of a sequence of discrete steps, interpreted as indicating a series of sharp, first-order phase transitions corresponding to the local melting of regions with successively increasing GC content.

One of the dominant approaches adopted in studies on DNA denaturation is the use of simplified models, which probe the gross, hopefully universal, features of the transition. Over the years, essentially two models have enjoyed widespread acceptance: the Poland-Scheraga (PS) model [12] and the Peyrard-Bishop (PB) model [13,14]. These models are not meant to provide a detailed theoretical description of the melting curve for any specific DNA molecule, although such extensions can and have been developed (see, for example, Refs. [15,16]). Rather, by being exactly soluble, they contribute to our understanding on a fundamental level by yielding universal features (such as the order of the transition, the role of self-avoidance, the size distribution of large loops, etc.) which are expected to be shared by more detailed and realistic microscopic models. A review of recent progress in the field can be found in Ref. [17].

The present paper investigates thermal denaturation in circular DNA within the framework of the PS model. In the PS model, and for the case of a homopolymer DNA, the molecule is represented by an alternating sequence of rigid bound segments and flexible denatured loops. Their contribution to the partition function are energetic and entropic, respectively. The entropy $S(l)$ of a loop of length l is of the form

$$e^{S(l)} \equiv \Omega(l) = A\,\frac{s^l}{l^c},$$

where A and s are constants and c is the *loop exponent* depending only on dimensionality and constraints imposed on the DNA chain such as excluded volume interactions. In the framework of the PS model, the nature of the transition is set by the value of c: for $c \leqslant 1$ no transition takes place and melting is just a gradual process in which the fraction of bound base pairs is nonzero at all temperatures; for $1 < c \leqslant 2$ the transition is of second order; for $c > 2$ it is of first order (i.e., the melting curve is discontinuous at the melting temperature T_c). It was shown relatively recently [18] that the excluded volume corrections in three dimensions yield $c \approx 2.12$. Therefore, the PS model predicts a first-order melting transition.

The DNA is a double helix and in order to open a denatured loop the region in which it is embedded must be unwound. This has no consequence for a linear DNA chain in thermal equilibrium, where the ends of the molecule are free to rotate. On the other hand, in circular DNA (such as plasmids) and in DNA with rotationally fixed ends the total *linking number* (LK), which measures the number of windings of one strand about the other, is conserved. In such cases the unwinding of one region must be compensated by the overwinding of another region.

Two mechanisms have been suggested to absorb the extra linking number in the overwound regions: (a) increasing of twist (Tw), or *overtwisting*, in which the change in the average stacking angle accounts for the extra windings [19,20], and (b) increasing of writhe (Wr), or *supercoiling*, where the backbone assumes a nonplanar shape that accommodates a nonzero LK [21–25]. The Călugăreanu-White-Fuller theorem implies that, during the melting process one has LK=Tw+Wr [26–29]. It has been shown that the two mechanisms have similar effects on the melting behavior: For $c \leqslant 2$, the melting process becomes a smooth crossover with no phase transition.

For $c > 2$, there is a phase transition of high order, where the singular part of the free energy scales with the reduced temperature $t \equiv (T - T_c)$ as $F_{\text{sing}} \sim |t|^{(c-1)/(c-2)}$. Thus the order of the transition diverges as c approaches 2 from above, and it becomes second order for $c \geqslant 3$. Unlike the full denaturation of DNA with free ends, the high-temperature phase here is composed of a critical fluid of microscopic loops coexisting with a single macroscopic loop [25].

In this paper, we investigate the general scenario where both mechanisms act simultaneously. We find that the nature of the transition is the same as that found in either of the two mechanisms separately. This observation is expected, although it is not guaranteed by the fact that the two limits (supercoiling or overtwisting alone) yield similar phase transition scenarios. To probe the interplay between supercoils and overtwist we also calculate the linking number absorbed by overtwist at the critical point.

The paper is organized as follows: In Sec. II the model is defined and analyzed with a formalism somewhat different from earlier accounts. In Sec. III the results are presented, first for simplified cases and then for the full model. We then conclude in Sec. IV with a brief discussion of our results.

II. MODEL

In order to incorporate supercoils and overtwist, we extend the PS model and assume that each configuration is composed of an alternating sequence of bound segments, loops, and supercoils, the latter being double-stranded chains, which carry writhe. It is assumed that supercoils form only within bound segments. Note that, localizing the writhe, inherently a nonlocal quantity, into well-defined supercoil regions is an approximation we employ here, in absence of an exact treatment otherwise. In very recent experiments on stretched DNA under torsional stress [30] localized supercoiled regions have been observed. Such configurations have also been used in recent theoretical studies of stretched DNA [31]. A typical configuration for our model is sketched in Fig. 1. The contribution of the three types of segments to the free energy can be computed the following rules.

(i) A bound segment of length l contributes to the internal energy $E_b < 0$ per unit length, and none to the entropy (due to the large persistence length of the double-stranded DNA).

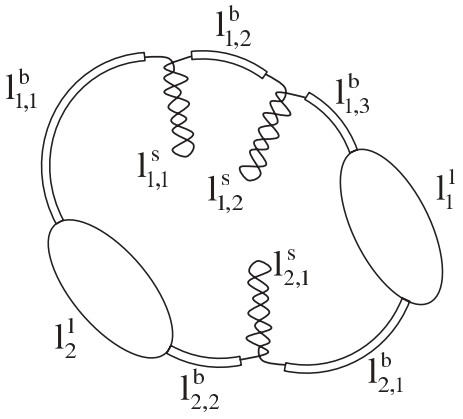

FIG. 1. A typical configuration of the model.

Hence, the associated Boltzmann weight is $e^{l\beta E_b} \equiv \omega^l$ with $\beta = 1/k_B T$.

(ii) A supercoil of length l contributes to the internal energy $E_s < 0$ per unit length with $E_s > E_b$, yielding a Boltzmann weight $e^{l\beta E_s} \equiv \nu^l$. It is assumed that like the bound segments, these segments carry no internal entropy although they do contribute to the overall entropy through their positional degree of freedom.

(iii) A loop of size l has an entropic contribution given by the Boltzmann weight $\Omega(l) = A\frac{s^l}{l^c}$. Here s is a geometry-dependent constant and A is a constant, usually termed the *cooperativity parameter*, reflecting both the normalization of the entropic contribution and the enthalpic cost of initiating a new loop.

In addition, we assume an overtwisting elastic energy cost with an elastic constant κ.

The excess linking number residing on the double-stranded DNA segments (bound segments and supercoils) is calculated as follows: A unit length of a loop region increases LK by 1, while a supercoil segment of the same length decreases LK by 1. We assume that all supercoils are uniform and identical in this respect (i.e., that a supercoil stem is wound uniformly around a central plectonemic axis and that the winding rate of all supercoiled regions is the same). Both of these assumptions have been used in past studies (see, for example [32]). The 1 : 1 ratio is adopted for the sake of simplicity, while considerations of universality suggest that the results should remain qualitatively unaltered under different choices. Denoting by L_b, L_s, and L_l the total length of the bound segments, supercoils, and loops, respectively, the excess LK in the double-stranded regions is simply $L_l - L_s$. This is compensated by an increase in the average stacking angle per unit length by $\Delta\theta$ in the bound segments and supercoils combined, hence $\Delta\theta = \frac{L_l - L_s}{L_b + L_s}$ [19]. Then, the elastic energy cost due to overtwisting is $\kappa(L_b + L_s)(\Delta\theta)^2 = \kappa\frac{(L_l - L_s)^2}{L_b + L_s}$, yielding the Hamiltonian

$$H = L_b\epsilon_b + L_s\epsilon_s + \kappa\frac{(L_l - L_s)^2}{L_b + L_s}.$$

Thus, for example, the Boltzmann weight of the configuration depicted in Fig. 1 is given by

$$\omega^{l^b_{1,1}}\nu^{l^s_{1,1}}\omega^{l^b_{1,2}}\nu^{l^s_{1,2}}\omega^{l^b_{1,3}}\Omega\left(l^l_1\right)\omega^{l^b_{2,1}}\nu^{l^s_{2,1}}\omega^{l^b_{2,2}}\Omega\left(l^l_2\right) \times e^{-\beta\kappa\frac{(l^l_1+l^l_2-l^s_{1,1}-l^s_{1,2}-l^s_{2,1})^2}{L-l^l_1-l^l_2}}.$$

It is worth noting that some of the previously studied PS-type models can be formulated as special cases of the present model: $L_s = 0$ corresponds to the case with overtwisting only [19]; $L_s = L_l$ corresponds to the case with supercoils only [23,25] and $\kappa = 0$ corresponds to a DNA with supercoils and no LK constraint [23].

The canonical partition function can now be written as

$$Z(L) = \sum_{L_b+L_l+L_s=L} Z_{\kappa=0}(L_b, L_l, L_s)e^{-\beta\kappa\frac{(L_l-L_s)^2}{L_b+L_s}}, \qquad (1)$$

where $Z_{\kappa=0}(L_b, L_l, L_s)$ is the partition sum with given $L_{b,l,s}$ and $\kappa = 0$ (which is an ensemble more restricted than even the microcanonical ensemble, as there may be different $L_{b,l,s}$

triplets that have the same energy). The correspondence with other models mentioned above can be obtained from Eq. (1) by taking the appropriate limits: The PS model is recovered when $\kappa = 0$ and $\nu = 0$ (or $E_s = \infty$ so that $L_s = 0$); taking $\nu = 0$, $\kappa > 0$ yields the partition sum for a model with overtwisting only [19]; finally, substituting $\kappa = \infty$, $\nu > 0$ recovers the case with supercoils only [23].

A. Free energy

We begin by calculating $Z_{\kappa=0}(L_b,L_l,L_s)$. This is conveniently done by first evaluating the grand canonical partition sum by means of a z transform of $Z_{\kappa=0}$. The canonical partition sum (expressed in terms of L_b,L_l, and L_s, or in terms of the fractions $m_i \equiv L_i/L, i = b,s,l$) is then calculated using the inverse transform. Introducing three fugacities, z_b,z_l, and z_s, corresponding to the three length constraints, the resulting grand canonical partition function $Q_{\kappa=0}(z_b,z_s,z_l)$ can be expressed in a closed form as

$$\begin{aligned} Q_{\kappa=0}(z_b,z_s,z_l) &= \sum_{L_{b,s,l}} Z_{\kappa=0}(L_b,L_s,L_l) z_b^{L_b} z_s^{L_s} z_l^{L_l} \\ &= 1 + \tilde{V}(z_b,z_s)U(z_l) \\ &\quad + \tilde{V}(z_b,z_s)U(z_l)\tilde{V}(z_b,z_s)U(z_l) + \cdots \\ &= \frac{1}{1-\tilde{V}(z_b,z_s)U(z_l)}, \end{aligned} \tag{2}$$

with

$$U(z_l) = A\sum_{l=1}^{\infty} \frac{s^l z^l}{l^c} = A\Phi_c(sz_l), \tag{3}$$

$$\begin{aligned} \tilde{V}(z_b,z_s) &= V(z_b) + V(z_b)W(z_s)V(z_b) + \cdots \\ &= \frac{V(z_b)}{1-W(z_s)V(z_b)}, \end{aligned} \tag{4}$$

$$V(z_b) = \sum_{l=1}^{\infty} \omega^l z_b^l = \frac{\omega z_b}{1-\omega z_b}, \tag{5}$$

$$W(z_s) = \sum_{l=1}^{\infty} \nu^l z_s^l = \frac{\nu z_s}{1-\nu z_s}. \tag{6}$$

The functions $U(z_l)$ and $\tilde{V}(z_b,z_s)$ are the grand canonical sums of single-stranded (loops) and double-stranded (bound and supercoiled) segments, respectively. Similarly, $V(z_b)$ and $W(z_s)$ denote the grand sums for bound and supercoiled segments, respectively. Here $\Phi_c(q)$ is the polylogarithm function of order c, which is analytic everywhere except for a branch cut for $q \geqslant 1$. The behavior of this function at $q = 1$ depends on c: If $c \leqslant 1$, $\Phi_c(q)$ diverges as $q \to 1^-$. If $c > 1$, $\Phi_c(q \to 1^-) = \zeta_c$ where ζ_c is the Riemann ζ function [33]. The behavior of $\Phi_c(q)$ near $q = 1$ determines the nature of the phase transition investigated here, as will be shown below. In deriving Eq. (2) we take $Z_{\kappa=0}(0,0,0) = 1$ and assume that the chain contains at least one loop and one bounded segment. This assumption simplifies the numerator of the resulting expression in (2) and it has no effect on the resulting thermodynamic properties of the model.

The canonical partition function is found by inverting the z transform using a Cauchy integral

$$Z_{\kappa=0}(L_b,L_l,L_s) = \left(\frac{1}{2\pi i}\right)^3 \oint \frac{Q_{\kappa=0}(z_b,z_s,z_l)}{z_b^{L_b+1} z_s^{L_s+1} z_l^{L_l+1}} dz_b dz_s dz_l. \tag{7}$$

All integration contours encircle the origin and contain no other singularities. Using Eqs. (2)–(6) we find

$$Q_{\kappa=0}(z_b,z_s,z_l) = \left[\frac{1}{\omega z_b} - \frac{1}{1-\nu z_s} - A\Phi_c(sz_l)\right]^{-1}.$$

$Q_{\kappa=0}$ has a simple pole in z_b set by

$$\frac{1}{\omega z_b} - \frac{1}{1-\nu z_s} - A\Phi_c(sz_l) = 0, \tag{8}$$

yielding

$$z_b^* = \frac{1}{\omega}\left[\frac{1}{1-\nu z_s} + A\Phi_c(sz_l)\right]^{-1}. \tag{9}$$

Note that Eq. (8) is equivalent to Eq. (2) in Ref. [25]. The z_b contour in Eq. (7) can be deformed to encircle the pole given by Eq. (9), yielding

$$Z_{\kappa=0}(m_b,m_l) = \left(\frac{1}{2\pi i}\right)^2 \oint e^{-L\tilde{F}_{\kappa=0}(z_s,z_l,m_b,m_l)} dz_l dz_s \tag{10}$$

with

$$\begin{aligned} \tilde{F}_{\kappa=0}(z_s,z_l,m_b,m_s) &= m_b \ln[z_b^*(z_s,z_l)] + m_s \ln(z_s) \\ &\quad + (1-m_b-m_s)\ln(z_l) \end{aligned} \tag{11}$$

up to logarithmic corrections in L. Here we used the fact that $m_b + m_s + m_l = 1$. In the thermodynamic limit the integral in Eq. (10) can be evaluated by considering the saddle point of $\tilde{F}_{\kappa=0}$ with respect to z_l and z_s,

$$0 = \frac{\partial \tilde{F}_{\kappa=0}}{\partial z_s} = -\frac{m_b \nu/(1-\nu z_s)}{1+(1-\nu z_s)A\Phi_c(sz_l)} + \frac{m_s}{z_s}, \tag{12}$$

$$\begin{aligned} 0 = \frac{\partial \tilde{F}_{\kappa=0}}{\partial z_l} &= -\frac{m_b(1-\nu z_s)A\Phi_{c-1}(sz_l)}{z_l\left[1+(1-\nu z_s)A\Phi_c(sz_l)\right]} \\ &\quad + \frac{1-m_b-m_s}{z_l}, \end{aligned} \tag{13}$$

where we used the identity $\frac{d}{dq}\Phi_c(q) = \frac{1}{q}\Phi_{c-1}(q)$. After some algebra Eq. (12) yields

$$z_s^* = \frac{1}{\nu}\left[1 + \frac{1+x-\sqrt{(1+x)^2+4x\eta}}{2\eta}\right], \tag{14}$$

where we define

$$x \equiv \frac{m_b}{m_s}, \quad \eta \equiv A\Phi_c(sz_l). \tag{15}$$

It can be seen (as $x,\eta > 0$) that $z_s^* < \nu^{-1}$, therefore the z_s integration contour can be deformed to pass through this saddle point without encircling the singularity of $\tilde{F}$ at $z_s = \nu^{-1}$. Eq. (13) yields

$$1 + \frac{A\Phi_{c-1}(sz_l)}{\frac{1}{1-\nu z_s^*} + A\Phi_c(sz_l)} = \frac{1}{m_b} - \frac{1}{x}. \tag{16}$$

The LHS of Eq. (16) is monotonically increasing with z_l (see Appendix A). For $c \leqslant 2$ this equation has a solution, z_l^*, for any value of m_b and x due to the fact that $\Phi_{c-1}(sz_l)$ diverges at $sz_l = 1$. However, for $c > 2$, the LHS reaches a finite value for $z_l = s^{-1}$ [the branch point of $\Phi_c(sz_l)$]. Therefore, for a given value of x, there is no saddle point for values of m_b below a critical threshold $m_b^{(c)}$ given by

$$m_b^{(c)}(x) = \left[1 + \frac{1}{x} + \frac{A\zeta_{c-1}}{\frac{1}{1-vz_s^*} + A\zeta_c}\right]^{-1}. \tag{17}$$

Here z_s^* is obtained using Eq. (14) with η replaced by $A\zeta_c$. For values $m_b < m_b^{(c)}(x)$ the z_l integral is equal to the value of the integrand at the branch point $z_l = s^{-1}$, as in the canonical treatment of the PS model [34]. The integration procedure involves more than simply evaluating the integrand at the singularity closest to the origin. Details are given in Appendix B.

To calculate the canonical partition function $Z(L)$ given in Eq. (1) the overtwist term should be added to the free energy, yielding

$$\begin{aligned}\tilde{F}(z_s,z_l,m_b,m_s) = {} & m_b \ln[z_b^*(z_s,z_l)] \\ & + m_s \ln(z_s) + (1 - m_b - m_s)\ln(z_l) \\ & + \beta\kappa \frac{(1 - m_b - 2m_s)^2}{m_b + m_s}.\end{aligned} \tag{18}$$

This full free energy needs to be minimized with respect to all of its arguments. The minimization with respect to z_s and z_l is the same as for $\tilde{F}_{\kappa=0}$ and the results are given by Eqs. (14) and (16). The minimization with respect to m_b and m_s is discussed in the next section.

In summary, the fugacities z_s,z_l in the thermodynamic limit (denoted by z_s^* and z_l^*) as functions of the bound and supercoiled segment fractions, m_b and m_s, are given by Eqs. (14) and (16). Hence we can express the Landau free energy, Eq. (18), as a function of the densities m_b and m_s only. In what follows it will be occasionally more convenient to express the dependence on m_s through the fraction $x = m_b/m_s$ as defined in Eq. (15). Then the Landau free energy can be written as

$$F(m_b,m_s) = F_{\kappa=0}(m_b,x) + \beta\kappa \frac{(1 - m_b - 2m_s)^2}{m_b + m_s}, \tag{19}$$

$$\begin{aligned}F_{\kappa=0}(m_b,x) &= \tilde{F}_{\kappa=0}[m_b,m_s,z_l(m_b,x),z_s(m_b,x)] \\ &= m_b \ln[z_b(z_s,z_l)] + \frac{m_b}{x}\ln[z_s(x,z_l)] \\ &\quad + \left(1 - m_b\frac{x+1}{x}\right)\ln(z_l),\end{aligned} \tag{20}$$

where z_b is given by Eq. (9), z_s is given by Eq. (14) and $z_l = z_l(m_b,x)$ is given by Eq. (16). Note that unlike other Landau free energies, which are analytic in the order parameter, here $F_{\kappa=0}(m_b,x)$ is a nonanalytic function of m_b and x along the line defined by $m_b^{(c)}(x)$. We shall denote this line of singularities by Γ. In the $m_b - m_s$ plane the expression for Γ is

$$(m_b,m_s) = \left(m_b^{(c)}(x), \frac{m_b^{(c)}(x)}{x}\right), \quad x \in (0,\infty). \tag{21}$$

For points to the left of Γ [i.e., those for which $m_b < m_b^{(c)}(x)$ so that $z_l = s^{-1}$] and for a given x the free energy is linear in m_b, while for points above Γ it has a more complicated form, hence $F_{\kappa=0}(m_b,m_s)$ is singular along Γ. Below we will explore this nonanalyticity in more detail and show that it is closely related to the nonanalytic behavior of the free energy as a function of temperature at the transition point.

III. RESULTS

After introducing the Landau free energy $F(m_b,m_s)$ and arguing that it is singular on a line (Γ) in the (m_b,m_s) plane, we move on to study the nature of the phase transition for different values of κ. Three cases are of interest.

(i) $\kappa = 0$: Here overtwisting has no cost and the chain is equivalent to a linear chain with supercoils freely spread within, with no linking number constraint. We will see that in this case the transition (which exists only for $c > 2$) is first order as in the standard PS model.

(ii) $\kappa = \infty$: Here overtwisting is forbidden. This is the case with supercoils only, which was analyzed in Ref. [25] and found to exhibit a continuous transition of order $\lceil \frac{c-1}{c-2} \rceil$ with a singularity in the free energy, which scales as $\sim t^{(c-1)/(c-2)}$. Here we will outline the derivation of this result within the current approach.

(iii) $0 < \kappa < \infty$: In this case supercoiling and overtwisting coexist, yielding a different free-energy minimum. Yet, it is shown that the nature of the transition remains the same as for $\kappa = \infty$.

To quantify the interplay between supercoiling and overtwisting, we calculate the fraction of the linking number accommodated by overtwist at the transition point

$$r(\kappa) \equiv m_{lc} - m_{sc} = 1 - m_{bc} - 2m_{sc}. \tag{22}$$

Clearly, $r(\kappa = \infty) = 0$ as no overtwist is allowed in this limit. Below we derive an explicit formula for $r(\kappa = 0)$ and calculate $r(0 < \kappa \leqslant \infty)$ numerically.

Throughout the paper the parameters used in the figures are $E_b = -3$, $E_s = -2$, $s = 5$, $A = 0.1$.

A. $\kappa = 0$

The densities m_s and m_b are found by minimizing $F(m_b,x) \equiv F_{\kappa=0}(m_b,x)$. This is equivalent to minimizing $\tilde{F}(z_s,z_l,m_b,m_s)$ with respect to all of its arguments, as F is obtained from $\tilde{F}$ by minimizing it with respect to the fugacities z_s and z_l. Using Eq. (20) and minimizing $F(m_b,m_s)$ yields

$$z_s(m_b,x) = z_l(m_b,x) = z_b(m_b,x), \tag{23}$$

i.e., the system is described by a single fugacity. This is expected, since for $\kappa = 0$ the grand canonical partition function of the full model could have been derived with a single fugacity corresponding to the single constraint $L_b + L_s + L_l = L$.

Substituting Eq. (23) in Eq. (20) one finds

$$F(T) = \ln\{z_l[m_b(T),x(T)]\},$$

where m_b, m_s and z_l can be calculated by solving Eqs. (9), (14), and (16) using Eq. (23). Hence the nonanalytic behavior of z_l results in a singularity in F. As mentioned above, for $c \leqslant 2$, $z_l(m_b,m_s)$ is an analytic function, therefore there is no phase

transition in the system. For $c > 2$, z_l increases monotonically from zero with temperature as long as $T < T_c$, where using Eq. (9) the critical temperature T_c is given by

$$\frac{1}{\omega(T_c)}\left[\frac{1}{1-\nu(T_c)/s}+A\zeta_c\right]^{-1}=\frac{1}{s}.$$

For $T > T_c$, $z_l = s^{-1}$ is a constant and hence $F(m_b,x)$ is constant, independent of T. As $T \to T_c$ from below, the free energy approaches the transition point with a nonzero slope, hence the transition is first order. This can be seen by differentiating Eq. (9) with respect to $T \sim \ln(\omega)$ using relation (23).

The equilibrium values of m_b and m_s as a function of T define a trajectory in the $m_b - m_s$ plane, as depicted in Fig. 2. The starting point of this trajectory at $T = 0$ is to the right of the singular line Γ since $m_b > m_b^{(c)}(x)$. As T increases, m_b decreases. At $T = T_c$ where the trajectory intersects Γ, the singular line defined above, a phase transition takes place.

The fact that the transition is first order can be verified as follows: the intersection of the trajectory with Γ takes place at a certain $x_c = m_{bc}/m_{sc}$ where m_{bc} and m_{sc} are the critical fractions of the bound segments and the supercoils on Γ, respectively. Since the minimum of the Landau free energy at the critical temperature is obtained at (m_{bc},m_{sc}), the slope of this free energy vanishes in all directions [i.e. $\partial F(m_{bc},x_c) = 0$]. As stated above and can been seen by

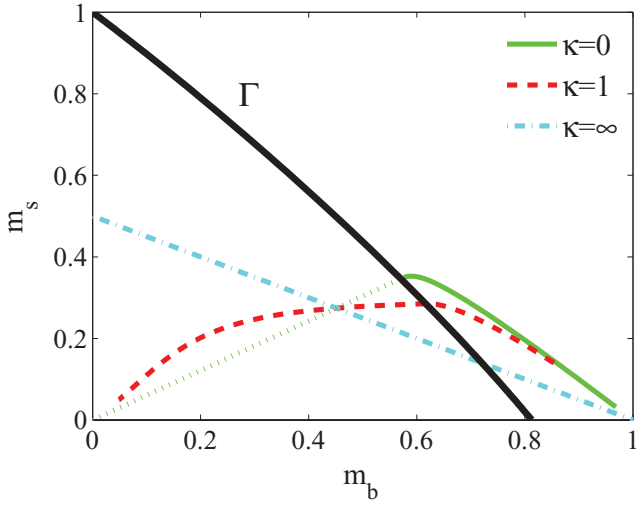

FIG. 2. (Color online) The (m_b,m_s) trajectories as a function of temperature of for $\kappa = 0$ (green full and dotted line), $\kappa = 1$ (red dashed line), and $\kappa = \infty$ (cyan dash-dotted line). For all lines $c = 2.5$. At $T = 0$ the chain is totally bound, so $m_b = 1$ and $m_s = 0$ for all trajectories. As T increases m_b decreases, intersecting at $T = T_c$ the singular line Γ [Eq. (21)], drawn above as a thick black line. On the $\kappa = 0$ trajectory there is a coexistence between a bound phase and a denaturated phase at $T = T_c$, along the dotted green line, while for $T > T_c$ the system is effectively unbound with $m_b = m_s = 0$. For $\kappa = 1$ (and any $\kappa > 0$) the trajectory continues smoothly across the singular line and reaches $m_b = m_s = 0$ only at $T = \infty$. For $\kappa = \infty$ the trajectory is linear due to the simple relation $m_s = \frac{1}{2}(1 - m_b)$.

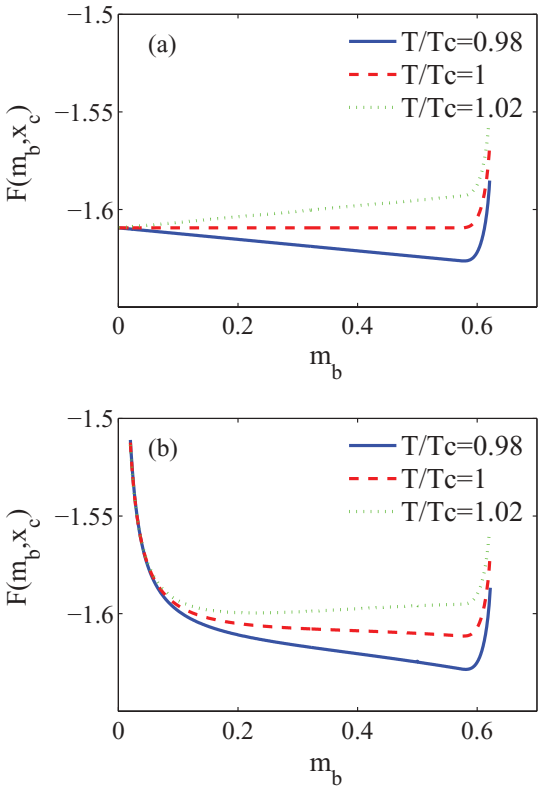

FIG. 3. (Color online) The Landau free energy $F(m_b,m_s)$ as defined in Eq. (19) along the line $m_b = x_c m_s$ where $x_c = \frac{m_{bc}}{m_{sc}}$, for $c = 2.5$ and (a) $\kappa = 0$; (b) $\kappa = 0.01$. While the free energy at the phase transition point for $\kappa = 0$ has a continuum of minima in the interval $0 \leqslant m_b \leqslant m_b^{(c)}(x)$, for $\kappa = 0.01$ (and for any $\kappa > 0$) there is a unique minimum of the free energy at all temperatures.

inspecting Eq. (20), for points to the left of Γ, where $m_b < m_{bc}$ and $T > T_c$, the free energy $F(m_b,x)$ is linear in m_b for fixed x. Hence the slope of $F(m_b,x_c)$ for $m_b < m_{bc}$ must be 0. This implies, in particular, that $F(m_{bc},x_c) = F(0,x_c)$, namely a phase coexistence between bound and unbound phases. Note that there is no free-energy barrier between the two phases. As depicted in Fig. 3(a) and can be verified by Eq. (20) above T_c the slope of $F(m_b,x_c)$ for $m_b < m_{bc}$ is positive and hence $m_b = m_s = 0$ is the minimal solution, so the system is in the unbound phase. As will be discussed below, setting $\kappa > 0$ eliminates the coexistence and yields a unique free-energy minimum at all temperatures [see Fig. 3(b)].

Let us now consider the overtwist linking number $r(\kappa = 0)$. The value of $x = m_b/m_s$ at criticality can be calculated using Eqs. (12) and (23)

$$x_c^{-1}=\frac{\nu s^{-1}/(1-\nu s^{-1})}{1+(1-\nu s^{-1})A\zeta_c}.$$

Solving Eq. (17) and $m_{sc} = m_{bc}x_c^{-1}$ for m_{bc} and m_{sc}, we obtain the overtwist linking number at T_c as

$$r(\kappa=0)=\frac{A\zeta_{c-1}(1-\nu s^{-1})^2-\nu s^{-1}}{1+(1-\nu s^{-1})^2(A\zeta_c+A\zeta_{c-1})}.$$

Depending on parameters in this expression, $r(\kappa = 0)$ can be either positive or negative. Specifically, for the parameters used

in Fig. 2 the value is $r(\kappa) = -0.26343 < 0$, implying that, the length of the supercoiled regions at the phase transition point exceeds the length needed to compensate for the linking number released by the loops, resulting in undertwisted bound segments.

B. $\kappa = \infty$

When $\kappa = \infty$, overtwisting is forbidden. The conservation of the linking number now implies $m_s = m_l$, therefore $m_s = \frac{1-m_b}{2}$. Minimizing Eq. (18) with respect to m_b and using the linking number constraint yields the relation

$$z_b = \sqrt{z_s z_l}, \tag{24}$$

which implies that two fugacities are needed, accounting for the two constraints on the linking number and the total chain length. Indeed, in previous accounts of this model the derivation was conducted using two fugacities [23,25]. Inserting Eq. (24) into Eq. (11) yields

$$F = \tfrac{1}{2}\ln(z_s) + \tfrac{1}{2}\ln(z_l) = \ln(z_b). \tag{25}$$

In Ref. [25] this case was analyzed and the transition was found to be of order $\lceil \frac{c-1}{c-2} \rceil$, which diverges as $c \to 2^+$, decreases as c increases and yields a second-order transition for $c \geqslant 3$. This can be seen by expanding Eqs. (12), (13), and (24) near the critical temperature, where $sz_l = 1$. Setting $t \equiv T_c - T$, $\delta m_b \equiv m_b - m_{bc}$, $\delta z_l \equiv z_l - s^{-1}$ and $\delta z_s = z_s - z_{sc}$, where m_{bc} and z_{sc} are the values of m_b and z_s at T_c, and using the identity $\Phi_c(1-\delta) \approx \zeta_c - \delta^{c-1}$ yields below the critical temperature ($t > 0$)

$$\delta m_b \sim \delta z_s \sim \delta z_l^{c-2} \sim t.$$

Hence $\delta z_l \sim t^{\frac{1}{c-2}}$. Expanding Eq. (25) to appropriate order in t and δz_l yields

$$\begin{aligned} F &= F(T_c) + \alpha t + \beta \delta z_l^{c-1} + O(t^2) \\ &\sim F(T_c) + \alpha t + \beta t^{\frac{c-1}{c-2}} + O(t^2). \end{aligned} \tag{26}$$

Above the critical temperature ($t < 0$) $\delta z_l = 0$ and hence the $\lceil \frac{c-1}{c-2} \rceil$th derivative of F diverges (or is discontinuous) at $T = T_c$, constituting a phase transition of the same order. The fact that the transition becomes more pronounced (of lower order) as the loop exponent c increases can be appreciated by inspecting Fig. 4 which shows m_b as function of temperature for c below and above 3.

C. $0 < \kappa < \infty$

In this case, as for $\kappa = 0$, both m_b and m_s are set by minimizing the Landau free energy given in Eq. (19). Here, however, there is no simple relation between the fugacities

$$\begin{aligned} 0 &= \frac{\partial F}{\partial m_b} \\ &= \ln\left[\frac{z_b}{z_l}\right] - \beta\kappa \frac{(1-m_b-2m_s)(1+m_b)}{(m_b+m_s)^2} \end{aligned} \tag{27}$$

$$\begin{aligned} 0 = \frac{\partial F}{\partial m_s} &= \ln\left[\frac{z_s}{z_l}\right] + \\ &- \beta\kappa \frac{(1-m_b-2m_s)(1+3m_b+2m_s)}{(m_b+m_s)^2}. \end{aligned} \tag{28}$$

These equations, together with Eqs. (14), (16) for $T \leqslant T_c$, and Eq. (14) and $z_l = s^{-1}$ for $T \geqslant T_c$, set the value of the order parameter m_b in the thermodynamic limit. Inserting Eqs. (27) and (28) into Eq. (18) yields

$$F(T) = \ln[z_b(m_b,m_s)] - \beta\kappa \frac{(1-m_b-2m_s)^2}{(m_b+m_s)^2}.$$

Repeating argument used for $\kappa = \infty$ shows that here, too, the order of the transition is $\lceil \frac{c-1}{c-2} \rceil$.

We observe in Fig. 2 that the trajectories for $\kappa = 0, 1, \infty$ in the (m_b, m_s) plane intersect at a single point (m_b^*, m_s^*). In fact, this special point is common to all such trajectories with arbitrary κ: Let T^* be the temperature for which the minimum of the free energy $F(m_b, m_s)$ satisfies $m_s^* = \frac{1-m_b^*}{2}$ for some κ. Then, for any other κ, the minimum of the free energy at T^* is also given by (m_b^*, m_s^*), because the κ-dependent part of the free energy $\kappa \frac{(1-m_b-2m_s)^2}{m_b+m_s}$ vanishes (and hence is minimal) when $m_s = \frac{1-m_b}{2}$.

We now consider the overtwist linking number at criticality for $0 < \kappa < \infty$. This number, $r = 1 - m_{bc} - 2m_{sc}$, cannot be obtained analytically. In Fig. 5 we present the numerically calculated $r(\kappa)/r(0)$ ratio for two values of c. $r(\kappa)$ depends weakly on c and could be either positive or negative, depending on the parameters of the model. However, for a given set of

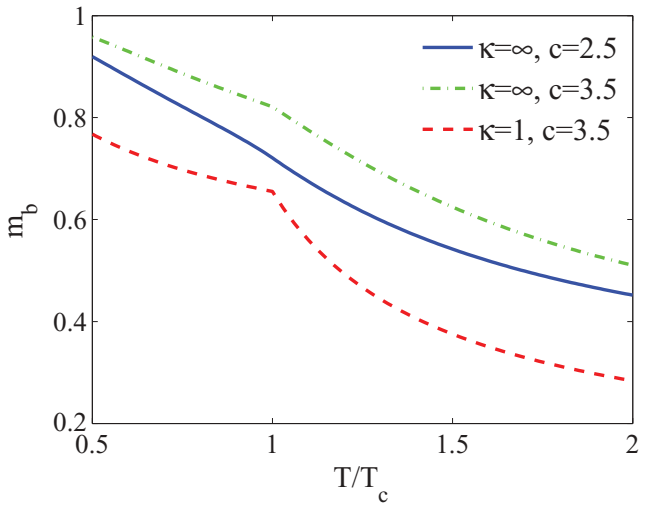

FIG. 4. (Color online) m_b vs. T for various c and κ. The signature of the second order transition is the non differentiability of the curves at $T = T_c$ when $c > 3$. For $2 < c < 3$ the melting curve is smooth with a higher order singularity at $T = T_c$. It can also be seen that the transition sharpens as κ decreases.

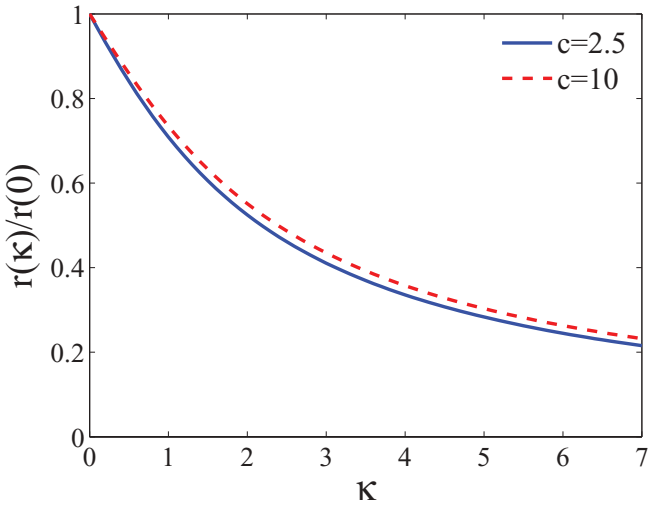

FIG. 5. (Color online) $r(\kappa)/r(0)$, where $r \equiv 1 - m_{bc} - 2m_{sc}$, for different values of c. It can be seen that $r(\kappa)/r(0)$ depends only weakly on c, and that, as expected, it decays monotonically from 1 for $\kappa = 0$ to 0 at $\kappa = \infty$.

parameters, the sign of $r(\kappa)$ does not change with κ. In order to demonstrate this point, consider the special point in Fig. 2 where all trajectories for different κ intersect at a shared temperature T^* and note that this point is the borderline between negative and positive $r(\kappa)$ on each trajectory. Therefore, if the parameters are such that the intersection is to the left of the singular line Γ, then for a given κ the critical temperature satisfies $T_c < T^*$ and hence $r(\kappa) < 0$. If, on the other hand, the intersection is to the right of the singular line then $r(\kappa) > 0$ for the same reason. In addition, if the parameters are such that the intersection is to the left of the singular line, a corollary follows that $T^* = T_c^{(\kappa=0)}$, which in turn implies $T_c^{(\kappa>0)} < T_c^{(\kappa=0)}$. Recalling that $\kappa = 0$ refers to the case with no LK conservation, this is in agreement with the experimental evidence that imposing circular topology reduces the melting temperature [22]. There is no equivalent statement in the other case in which the intersection is to the right of the singular line.

IV. CONCLUSION

In this paper we analyzed the thermal denaturation of a circular DNA molecule, in which the linking number is conserved. Within the framework of the Poland-Scheraga model, we have considered the two possible mechanisms for conserving the LK: writhing (forming supercoils) and overtwisting. The denaturation transition is studied for arbitrary values of the elastic constant κ associated with the overtwist elastic energy. We found that the model exhibits no transition for $c \leqslant 2$ and a high-order, continuous transition for $c > 2$, $\kappa > 0$. The singular part of the free energy was found to scale as $t^{\frac{c-1}{c-2}}$ with $t = T_c - T$, yielding a transition of order $\lceil \frac{c-1}{c-2} \rceil$. The order of the transition diverges as c approaches 2 from above, it decreases with increasing c and it becomes second order for $c \geqslant 3$. The model with $\kappa = 0$ behaves differently, exhibiting no transition for $c \leqslant 2$ and a first-order transition for $c > 2$. Similar observations were reported before for the limiting cases restricted to supercoils only [25] and overtwist only [35].

The canonical analysis carried out here brings new insights. For example, the first-order transition that takes place for $\kappa = 0$ and $c > 2$ is found to be rather special in that it does not have a metastable region [see Fig. 3(a)]. This is true also for the original PS model. In addition, the analysis of the (m_b,m_s) trajectories unveiled a κ-independent special point (m_b^*,m_s^*), which in return led to the prediction that $T_c^{(\kappa>0)} < T_c^{(\kappa=0)}$ (the melting temperature reduced by circular topology) for a wide range of parameters, in line with an earlier experimental observation.

The model considered in this paper corresponds to a homogeneous circular DNA chain, while biological DNA molecules are heterogeneous. However, through the Harris criterion [36] we find that the disorder is irrelevant for $\kappa > 0$ and $c < 3$, where the specific heat exponent $\alpha = 2 - \frac{c-1}{c-2} = \frac{c-3}{c-2}$ is negative. Therefore we do not expect the sequence heterogeneity to change the nature of the phase transition and the associated critical exponents. As the actual value of the loop exponent was estimated to be $c \approx 2.12$ [18], our analysis should be valid for sufficiently long, real DNA chains.

Previous accounts on denaturation of circular DNA have found that a macroscopic loop is formed above T_c, reminiscent of Bose-Einstein condensation. Although not discussed here, we expect a similar phenomenon in the combined model of supercoils and overtwist, and it would be interesting to analyze the linking number exchange between the macroscopic loop, the microscopic loops, and the supercoiled and overtwisted segments.

ACKNOWLEDGMENTS

We thank O. Cohen, O. Hirschberg, S. Medalion, and Y. Rabin for helpful discussions. This work was supported by the Israel Science Foundation (ISF) and the Turkish Technological and Scientific Research Council (TUBITAK) through the grant TBAG-110T618.

APPENDIX A: MONOTONICITY OF THE RHS OF EQ. (16)

We wish to show that

$$f(z_l) = \frac{A\Phi_{c-1}(sz_l)}{\frac{1}{1-\nu z_s} + A\Phi_c(sz_l)}$$

is a monotonically increasing function for $z_l \in (0,s^{-1})$. Using Eq. (14) we can write

$$g(\eta,x) \equiv \frac{1}{\eta}\frac{1}{1-\nu z_s(z_l,x)} = \frac{2}{\sqrt{(1+x)^2+4x\eta}-(1+x)},$$

where $\eta = A\Phi_c(sz_l)$ increases and $g(\eta,x)$ decreases with z_l. Hence we can write

$$f(z_l) = \frac{1}{1+g(\eta,x)} \times \frac{\Phi_{c-1}(sz_l)}{\Phi_c(sz_l)},$$

where the first factor is an increasing function of z_l. It is thus sufficient to show that the second factor also increases with z_l.

To this end, we differentiate this term

$$\frac{d}{dz_l}\left[\frac{\Phi_{c-1}(sz_l)}{\Phi_c(sz_l)}\right] = \left[\frac{\Phi_{c-2}(sz_l)\Phi_c(sz_l)}{\Phi_c(sz_l)^2} - \frac{\Phi_{c-1}(sz_l)^2}{\Phi_c(sz_l)^2}\right].$$

Now we show that the numerator of the derivative, denoted by $\Sigma(z_l)$ is positive, by expressing the polylogarithm function explicitly as a power series of the variable $y = sz_l$,

$$\begin{aligned}\Sigma(z_l) &= \sum_{k,l=1}^{\infty}\left[\frac{y^l}{l^{c-2}}\frac{y^k}{k^c} - \frac{y^l}{l^{c-1}}\frac{y^k}{k^{c-1}}\right] \\ &= \sum_{k,l=1}^{\infty}\frac{y^l}{l^{c-1}}\frac{y^k}{k^c}[l-k] \\ &= \sum_{k<l}^{\infty} y^{l+k}[l-k]\left[\frac{1}{l^{c-1}}\frac{1}{k^c} - \frac{1}{k^{c-1}}\frac{1}{l^c}\right] \\ &= \sum_{k<l}^{\infty}\frac{y^{l+k}}{l^c k^c}[l-k]^2 > 0.\end{aligned}$$

This demonstrates that $f(z_l)$ is a monotonically increasing function of z_l.

APPENDIX B: BRANCH-CUT INTEGRATION

We wish to evaluate the integral for the partition function with $\kappa = 0$ given in Eq. (10)

$$\psi(L_b,L_s,L_l) = \frac{1}{2\pi i}\oint e^{-L\tilde{F}_{\kappa=0}(z_s,z_l,m_b,m_s)}dz_l,$$

with $z_s(x,z_l)$ given by Eq. (14). L_i satisfy $L_b + L_l + L_s = L$, $L_b/L_s = x$ and $m_i = L_i/L$ $(i = b,s)$. Defining $y = sz_l$ yields

$$\begin{aligned}\psi(L_b,x) &= \frac{s^{L_l}}{2\pi i}\oint \frac{\left[\frac{1}{1-\nu z_s} + A\Phi_c(y)\right]^{L_b}}{z_s^{L_b/x}\, y^{L-L_b\frac{1+x}{x}}}dy \\ &= \frac{s^{L_l}}{2\pi i}\oint I(y)^L dy.\end{aligned}$$

Equation (17) defines the value of $m_b = L_b/L$ below which the integrand has no saddle point, therefore the integral should be evaluated by another method. The integration contour can be deformed to the contour depicted in Fig. 6, composed of the following segments:

$$\begin{aligned}&\text{(I)} : [R - i\epsilon, 1 - i\epsilon] \\ &\text{(II)} : \left\{1 - \epsilon e^{i\theta} : \frac{\pi}{2} < \theta < \frac{3\pi}{2}\right\} \\ &\text{(III)} : [1 + i\epsilon, R + i\epsilon] \\ &\text{(IV)} : \{Re^{i\theta} : \delta < \theta < 2\pi - \delta\},\end{aligned} \tag{B1}$$

where $R \to \infty$ and $tg(\delta) = \frac{\epsilon}{R}$. We wish to show now that the only contribution comes from the vicinity of the branch point: To see that the contribution of (IV) is negligible we note that for $|y| \to \infty, |\Phi_c(y)| \to \frac{\ln(y)^c}{\Gamma(c+1)}$ [37]. From Eq. (14) we see that for $|y| \to \infty z_s \to 1$ and $\frac{1}{1-\nu z_s} \to \sqrt{\Phi_c(y)}$ so that

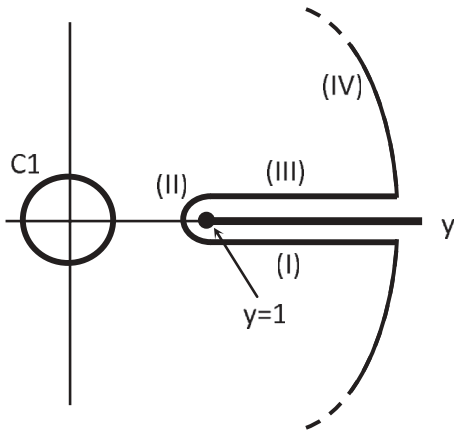

FIG. 6. The original contour of integration C1 can be deformed to the contour, which is given by Eq. (B1) and is described in the text of Appendix B. The branch point $y = 1$ is marked here by a filled circle.

for large enough L and $x < \infty$,

$$\lim_{R\to\infty}[I(Re^{i\theta})]^L \sim \lim_{R\to\infty}\frac{\ln(R)^{cL_b}}{R^{L-L_b\frac{1+x}{x}}} < \lim_{R\to\infty}\frac{1}{R^2}.$$

Hence segment (IV) of the contour has no contribution. Along segment (II) the function $I(y)$ is analytic and hence the integral is of order ϵ and can be taken to be arbitrarily small.

$I(y)$ can be written as a power series with only real coefficients, and hence $I(y^*)^L = I^*(y)^L$, where y^* is the complex conjugate of z. Integrating along segments $(I) + (III)$ yields

$$\psi = \frac{s^{L_l}}{2\pi i}\int_{(I)+(III)} I(y)^L dy = \frac{s^{L_l}}{\pi}\int_1^{\infty}\mathrm{Im}[I(y)^L]dy.$$

Defining $I(y) = \Lambda(y)e^{i\Psi(y)}$, where $\Lambda(y)$ and $\Psi(y)$ are real functions, we can write $\mathrm{Im}[I(y)^L] = \Lambda(y)^L \sin[L\Psi(y)]$. As $\Psi(y)$ is a smooth function for $y > 1$ in the thermodynamic limit the oscillations in the sin() function average out to zero. Therefore, the only contribution to the integral comes from the vicinity of $y = 1$, where $\Psi(y)$ has a discontinuity in some derivative.

The function $I(y)$ has a pole at $y = 0$ where $I(y \to 0_+) \to \infty$, so that $I'(y) < 0$ near the origin. When $c > 2$, the fact that there is no saddle point for $0 < y < 1$ implies that $I'(1) < 0$ as well, and hence $\Lambda'(1) < 0$. For $\delta y \equiv y - 1 \ll 1$ the imaginary part of the polylogarithm function is approximately $\mathrm{Im}[\Phi_c(1+\delta y)] \approx a\delta y^{c-1}$ with $a = \pi/\Gamma(c)$, and therefore $\Psi(1+\delta y) \approx \tilde{a}\delta y^{c-1}$ with $\tilde{a} = [a/\Lambda(1)]) \times \partial I/\partial\Phi_c(y)$. Combining these observations yields to leading order $I(1+\delta y) \approx \Lambda(1)\exp[-b\delta y + i\tilde{a}\delta y^{c-1}]$ with $b = -\Lambda'(1)/\Lambda(1) > 0$.

$$\psi \approx \frac{s^{L_l}}{\pi}\Lambda(1)^L\int_0 e^{-bL\delta y}\sin(L\tilde{a}\delta y^{c-1})d\delta y.$$

The contribution to the integral comes from a region of size $\delta y \sim \frac{1}{L}$, so that the upper limit can be stretched to ∞ without affecting the result. Rescaling by $\tilde{y} = bL\delta y$ we obtain

$$\psi \approx \frac{s^{L_l}}{\pi}\Lambda(1)^L(bL)^{-1}\int_0^{\infty} e^{-\tilde{y}}\sin\left(\frac{\tilde{a}\tilde{y}^{c-1}}{b^{c-1}L^{c-2}}\right)d\tilde{y}.$$

As $c > 2$, in the thermodynamic limit $L \to \infty$ the argument of the sin() function is small and it can be expanded.

$$\psi \approx \frac{\tilde{a}(bL)^{c-2}}{\pi L} s^{L_l} \Lambda(1)^L \int_0^\infty e^{-\tilde{y}} \tilde{y}^{c-1} d\tilde{y} = \frac{\tilde{a}(bL)^{c-2}\Gamma(c)}{\pi L} s^{L_l} \Lambda(1)^L .$$

Substituting back $z_l = y/s$ yields

$$\psi(L_b, L_s, L_l) \approx \frac{\tilde{a}(bL)^{c-2}\Gamma(c)}{\pi L} e^{-L\tilde{F}_{\kappa=0}(z_l = s^{-1}, z_s, m_b, m_s)},$$

where $z_s = z_s(z_l, x)$ is given in Eq. (14). Hence up to logarithmic corrections the free energy is given by its value at the branch point.

[1] H. Hiasa and K. Marians, J. Biol. Chem. **269**, 32655 (1994).
[2] H. Hiasa and K. Marians, J. Biol. Chem. **271**, 21529 (1996).
[3] D. Dixon, R. Simpson-White, and L. Dixon, J. Mar. Biol. Assoc. UK **72**, 519 (1992).
[4] D. Hickey and G. Singer, Genome Biology **5**, 117 (2004).
[5] R. M. Wartell and A. S. Benight, Phys. Rep. **126**, 67 (1985).
[6] R. D. Blake and S. G. Delcourt, Nucleic Acids Res. **26**, 3323 (1998).
[7] P. Baaske, S. Duhr, and D. Braun, Appl. Phys. Lett. **91**, 133901 (2007).
[8] G. Bonnet, O. Krichevsky, and A. Libchaber, Proc. Natl. Acad. Sci. USA **95**, 8602 (1998).
[9] G. Altan-Bonnet, A. Libchaber, and O. Krichevsky, Phys. Rev. Lett. **90**, 138101 (2003).
[10] A. Hanke and R. Metzler, J. Phys. A **36**, L473 (2003).
[11] T. Ambjörnsson, S. K. Banik, O. Krichevsky, and R. Metzler, Biophys. J. **92**, 2674 (2007).
[12] D. Poland and H. A. Scheraga, J. Chem. Phys. **45**, 1456 (1966).
[13] M. Peyrard and A. R. Bishop, Phys. Rev. Lett. **62**, 2755 (1989).
[14] T. Dauxois, M. Peyrard, and A. R. Bishop, Phys. Rev. E **47**, R44 (1993).
[15] R. D. Blake *et al.*, Bioinformatics **15**, 370 (1999).
[16] R. Blossey and E. Carlon, Phys. Rev. E **68**, 061911 (2003).
[17] J. Phys.: Condens, Matter **21**(3) (2009), special section on DNA melting, edited by R. Blossey.
[18] Y. Kafri, D. Mukamel, and L. Peliti, Phys. Rev. Lett. **85**, 4988 (2000).
[19] J. Rudnick and R. Bruinsma, Phys. Rev. E **65**, 030902(R) (2002).
[20] T. Garel, H. Orland, and E. Yeramian, arXiv:q-bio/0407036 (2004).
[21] L. Yan and H. Iwasaki, Jpn. J. Appl. Phys. **41**, 7556 (2002).
[22] V. Víglaský, M. Antalík, J. Adamcík, and D. Podhradský, Nucleic Acids Res. **28**, e51 (2000).
[23] A. Kabakçıoğlu, E. Orlandini, and D. Mukamel, Phys. Rev. E **80**, 010903(R) (2009).
[24] A. Kabakçıoğlu, E. Orlandini, and D. Mukamel, Physica A (Amsterdam) **389**, 3002 (2010).
[25] A. Bar, A. Kabakçıoğlu, and D. Mukamel, Phys. Rev. E **84**, 041935 (2011).
[26] G. Călugăreanu, Rev. Math. Pures Appl **4**, 5 (1959).
[27] G. Călugăreanu, Czechoslovak Math. J. **11**, 588 (1961).
[28] J. White, Am. J. Math. **91**, 693 (1969).
[29] F. Fuller, Proc. Natl. Acad. Sci. **68**, 815 (1971).
[30] M. T. J. van Loenhout, M. V. de Grunt, and C. Dekker, Science **338**, 94 (2012).
[31] J. F. Marko and S. Neukirch, Phys. Rev. E **85**, 011908 (2012).
[32] J. F. Marko and E. D. Siggia, Phys. Rev. E **52**, 2912 (1995).
[33] M. Abramowitz and I. Stegun, *Handbook of Mathematical Functions*, 5th ed. (Dover, New York, 1964).
[34] F. W. Wiegel, in *Conformational Phase Transition in a Macromolecule: Exactly Solvable Models, Phase Transitions and Critical Phenomena*, Vol. 7 (Academic, New York, 1983), p. 101.
[35] A. Kabakçıoğlu, A. Bar, and D. Mukamel, Phys. Rev. E **85**, 051919 (2012).
[36] A. B. Harris, J. Phys. C **7**, 1671 (1974).
[37] L. Lewin, *Polylogarithms and Associated Functions* (North-Holland, New York, 1981).